

# Diagonal superexchange in a simple square CuO<sub>2</sub> lattice

V. A. Gavrichkov,<sup>1,2</sup> S. I. Polukeev,<sup>1</sup> and S. G. Ovchinnikov<sup>1</sup>

<sup>1</sup>*Kirensky Institute of Physics, Siberian Branch of the Russian Academy of Sciences, 660036 Krasnoyarsk, Russia*

<sup>2</sup>*Rome International Center for Materials Science Superstripes RICMASS, via del Sabelli 119A, 00185, Roma, Italy*

(Dated: January 30, 2025)

Many microscopic models with interaction between the next-nearest neighbours as a key parameter to cuprate physics inspired us to study here the diagonal superexchange interaction in the CuO<sub>2</sub> layer. Our investigation shows the models with extended hopping give a correct representation of magnetic interactions only in a hypotheticalal square CuO<sub>2</sub> layer, where the diagonal superexchange interaction with the next-nearest neighbours neighbors always has the AFM nature. The conclusions are based on the presence of a symmetry prohibition on the FM contribution to the total diagonal superexchange between the next-nearest neighbors for a simple square CuO<sub>2</sub> layer, but not for the real CuO<sub>2</sub> layer. We actually confirm also there are justified reasons to consider magnetic frustrations and high sensitivity of spin nanoinhomogeneity to a breaking square symmetry.

## I. INTRODUCTION

A theory of superexchange interaction qualitatively and quantitatively describes well the antiferromagnetic (AFM) interaction of nearest neighbor ions Cu<sup>2+</sup> in the CuO<sub>2</sub> layer of the parent cuprates (see works <sup>1-3</sup> and references therein) including pressure and optical pumping effects <sup>4,5</sup>. However, a nature of hopping and superexchange with the next-nearest neighbors is less obvious and has being under discussion for a long time <sup>6-10</sup>.

These parameters are relevant in many approaches to studying the physics of high- $T_c$  superconducting (HTSC) cuprates. The hopping and superexchange with the next-nearest neighbors could be important not only for the extended hopping problem in the set of  $t$ - $J$ ,  $t$ - $t'$ - $J$ ,  $t$ - $t'$ - $t''$ - $J$  models with a realistic hole pairing mechanism in the HTSC cuprates (see <sup>11</sup> and references therein) but also for understanding a nature of a pseudogap state with  $\vec{k}$  arcs in the antinodal direction of the Fermi surface in  $\vec{k}$ -dependent experiments<sup>12,13</sup>. Moreover, it is known the temperature window for the pseudogap state shrinks with the increasing next-nearest neighbor hopping, which indicates that the diagonal hopping may not be supportive to the pseudogap features <sup>14</sup>. Results of dynamic cluster quantum Monte Carlo simulations for the Lifshitz transition of the two-dimensional Hubbard model show sensitivity to a magnitude of the diagonal next-nearest neighbor hopping as control parameter <sup>15</sup>. Complicated spectral features of the two-dimensional Hubbard model are simply interpreted near the Mott transition, by considering how the next-nearest neighbor hopping shifts the spectral weights<sup>16</sup>. The momentum-sector-selective metal-insulator transitions in the eight-site dynamical cluster approximation for the 2D Hubbard model are explored on the phase diagram in the space of interaction and second-neighbor hopping control parameters <sup>17</sup>. The magnitude of diagonal neighbors interaction plays a key role in the study of spin (SDW) and charge(CDW) nanoinhomogeneity in the cuprate material, where both observed phases have tilted stripes (so called "Y shift") with the same degree of tilting <sup>10</sup>, and the origin of the

tilting can be explained by a small anisotropy in the hopping between the next-near neighbors. The specific alignment direction of the stripes is so sensitive to the hopping interaction where even a small anisotropy in the one can result in the subtle observed tilting in LSCO <sup>6,18,19</sup> and LBCO <sup>20</sup> samples.

However, the studies of the effects of the next-nearest neighbor hopping and magnetic frustrations on the spectrum of quasiparticles are still based on some assumptions regarding the sign and magnitude of the hopping and superexchange interaction  $J_{tot}(\vec{R}_{11})$  between the diagonal neighbors. This is certainly not enough to understand the whole range of phenomena associated with these parameters. In previous papers <sup>4,21</sup> we derived a simple rule for detecting the sign of the contribution to the superexchange interaction from a single virtual electron-hole pair. However, our conclusions concerned only the interaction with the nearest neighboring magnetic ions. For the CuO<sub>2</sub> layer of parent cuprates, this magnitude  $J_{tot}(\vec{R}_{01}) \approx 0.15eV$  <sup>5</sup> is in the agreement with the neutron scattering data <sup>3</sup>, and the approach itself allows us to study the dependence of the superexchange in the 3d oxides on external factors: applied pressure<sup>5,21</sup> and optical pumping <sup>22</sup>.

In parent cuprates, the virtual hopping and electron-hole pairs at the (next-)nearest neighbors can also lead to superexchange between them. We showed here the superexchange parameter  $J_{tot}(\vec{R}_{ij})$ , important for other approaches, behaves in an unusual way. Indeed, it has a zero magnitude at the diagonal directions  $\vec{R}_{ij} = \vec{R}_{11}$  of the square CuO<sub>2</sub> layer for the virtual electron-hole pair with  $B_{1g}$  hole symmetry, where the corresponding <sup>3</sup> $B_{1g}$  triplet band competes in energy with the Zhang-Rice singlet <sup>1</sup> $A_{1g}$  band <sup>5,23-25</sup>. This leads exactly to a zero FM contribution to the total magnetic interaction  $J_{tot}(\vec{R}_{11})$  between next-nearest neighbors of Cu<sup>2+</sup> ions. As a consequence, the latter has a purely AFM nature  $J_{tot}(\vec{R}_{11}) < 0$ , but quickly decreases with distance between the Cu<sup>2+</sup> ions.

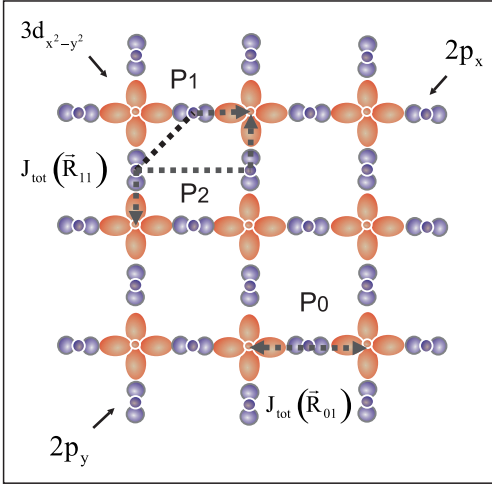


FIG. 1. Paths  $P_0$ ,  $P_1$  and  $P_2$  of superexchange interactions  $J_{tot}(\vec{R}_{01})$  and  $J_{tot}(\vec{R}_{11})$  for the first and the second neighbor ions with the participation of  $2p$  oxygen orbitals forming  $\sigma$  overlapping with  $3d$  copper ions, and  $90^\circ$  ( $P_1$ ) or small  $\pi$  ( $P_2$ ) - overlapping between themselves. Here the interactions  $J_{tot}(\vec{R}_{01})$  is of AFM nature, but magnitudes of the  $J_{tot}(\vec{R}_{11})$  interaction with second neighbors is still unknown.

The paper is organized as follows: in next section (Sec.II), we provide some theoretical background on the manyelectron approach to the study of superexchange interaction in the parent cuprates. Details of symmetric effects on superexchange in  $\text{CuO}_2$  layer with the square symmetry appear in Sec.III. We discussed and conclude in Sec.IV

## II. HAMILTONIAN

In this section, we investigate the sign and magnitude of the superexchange interaction  $J_{tot}(\vec{R}_{11})$  with next-nearest-neighbor  $\text{Cu}^{2+}$  ions through different oxygen orbitals in the  $\text{CuO}_2$  layer (see Fig.1). Indeed, in the magnetic interaction with second neighbors, the overlapping oxygen orbitals play a significant role. There are two paths  $P_1$  and  $P_2$  to create a various virtual electron-hole pairs. They are distinguished by the overlapping oxygen orbitals. There are the  $90^\circ$  degree overlapping oxygen orbitals on the path  $P_1$ , and the small  $\pi$  - overlapping at the path  $P_2$ . The virtual electron-hole pairs in both paths can generate both AFM and FM contributions to the superexchange interaction  $J_{tot}(\vec{R}_{11})$  between the diagonal second neighbor  $\text{Cu}^{2+}$  ions.

The exchange parameter  $J_{tot}(\vec{R}_{ij})$  in Eq.(1) is additive over all possible states in the electronic  $N_+$  ( $|A_1\rangle$ ) and two-hole  $N_-$  ( $|^1A_{1g}\rangle_{nS}, |^3B_{1g}\rangle_{mT}, \dots$ ) sectors in Fig.2, and the superexchange interaction (1) is obtained in second order of a cell perturbation theory over interband contributions to the total Hamiltonian  $\hat{H}$  from the interatomic hopping contribution<sup>4,26,27</sup>.

$$\hat{H}_S = \hat{H}_{AFM} + \hat{H}_{FM}, \quad (1)$$

where  $\hat{H}_{AFM} = \sum_{ij} J_{AFM}(\vec{R}_{ij}) (\vec{s}_i \vec{s}_j - \frac{1}{4} n_i n_j)$ ,  $\hat{H}_{FM} = \sum_{ij} J_{FM}(\vec{R}_{ij}) (\vec{s}_i \vec{s}_j + \frac{3}{4} n_i n_j)$ , and the exchange constants  $J_{AFM}(\vec{R}_{ij}) > 0$ ,  $J_{FM}(\vec{R}_{ij}) < 0$  are given by

$$J_{AFM}(\vec{R}_{ij}) = \sum_{nS} J_{AFM}^{(nS)}(\vec{R}_{ij}) = \sum_{nS=1}^{N_S} |t^{0,nS}(R_{ij})|^2 / \Delta_{nS}, \quad \Delta_{nS} = E_{nS} + E_{1A} - 2\varepsilon_{b_{1g}} \quad (2)$$

$$J_{FM}(\vec{R}_{ij}) = \sum_{mT} J_{FM}^{(mT)}(\vec{R}_{ij}) = - \sum_{mT=1}^{N_T} |t^{0,mT}(R_{ij})|^2 / 2\Delta_{mT}, \quad \Delta_{mT} = E_{mT} + E_{1A} - 2\varepsilon_{b_{1g}}.$$

The total multielectron Hamiltonian in the representa-

tion of the Hubbard operators<sup>28</sup>, looks like  $\hat{H} = \hat{H}_0 + \hat{H}_1$ ,<sup>29,30</sup> where

$$\hat{H}_0 = \sum_i \left\{ (E_{1A^1A} - N_+ \mu) X_i^{1A^1A} + (\varepsilon_{b_{1g}} - N_0 \mu) X_i^{b_{1g} b_{1g}} + \sum_{h=nS, mT} (E_h - N_- \mu) X_i^{hh} \right\} \quad (3)$$

$$\hat{H}_1 = \sum_{ij\sigma} \sum_{rr'} t_{\sigma}^{rr'}(\vec{R}_{ij}) X_i^{+r} X_j^{r'}$$

$$t_{\sigma}^{r,r'}(\vec{R}_{ij}) = \sum_{ij} \sum_{\lambda\lambda'} \sum_{rr'} t_{\lambda\lambda'}(\vec{R}_{ij}) \gamma_{\lambda\sigma}^*(r) \gamma_{\lambda'\sigma}(r'),$$

and  $\gamma_{\lambda\sigma}^*(r) = \langle h|c_{\lambda\sigma}^+|b_{1g}\rangle$ , where the index  $h$  runs over all possible two-hole states in the  $N_-$  sector for the material with magnetic ions  $\text{Cu}^{2+}$  in the  $d^9$  electron configuration. Here,  $X_i^{+r} = |h\rangle\langle b_{1g}|(|^1A\rangle\langle b_{1g}|)$  is Hubbard operators of hole(electron) creation with root vectors  $r = (h, b_{1g})$ . Virtual electron-hole excitations through the dielectric gap  $\Delta_h = E_h + E_{1A} - 2\varepsilon_{b_{1g}}$  to the conduction band and vice versa in Eq.(2) contribute to the superexchange interaction  $\hat{H}_S$  <sup>4</sup>:

$$\begin{aligned} t^{0,nS}(R_{ij}) &\equiv t^{(^1Ab_{1g}), (b_{1g}nS)}(R_{ij}) = \\ &= \sum_{\lambda\lambda'} t^{\lambda\lambda'}(R_{ij}) \gamma_{\lambda\sigma}^*(^1Ab_{1g}) \gamma_{\lambda'\sigma}(b_{1g}nS) \\ t^{0,mT}(R_{ij}) &\equiv t^{(^1Ab_{1g}), (b_{1g}mT)}(R_{ij}) = \\ &= \sum_{\lambda\lambda'} t^{\lambda\lambda'}(R_{ij}) \gamma_{\lambda\sigma}^*(^1Ab_{1g}) \gamma_{\lambda'\sigma}(b_{1g}mT). \end{aligned} \quad (4)$$

The spin Hamiltonian (1) was derived from the original Hamiltonian (3) by using the projective operator method <sup>4,27</sup>. For details of the derivation of the multielectron Hamiltonian from the multi-orbital  $pd$  model, see the works<sup>31-33</sup>, where a five-orbital basis  $p_\lambda, (\lambda = x, y, z), d_{x^2-y^2}, d_{z^2}$  was typically used. All possible eigenstates  $|^1A_{1g}\rangle_{nS}$  and  $|^3B_{1g}\rangle_{mT}$  in the configuration space in Fig.2, as well as their energies  $E_h$  with  $h = nS, mT$  are obtained in the exact diagonalization procedure for the intra-cell part of multi-orbital  $pd$  model <sup>33</sup>. The sum of all FM and AFM contributions corresponds to the sum over all possible virtual electron-hole pairs (so called exchange loops <sup>21</sup>). The FM or AFM nature of the contribution from a specific exchange loop is easily determined using the rule: if  $S_+ = S_-$  is an AFM contribution, in the case of  $S_+ = S_- \pm 1$  is an FM contribution, where  $S_\pm$  is the spin of the electron and hole in the specific virtual pair <sup>21,34</sup>[25,38]. The all triplet states  $|mT\rangle$  in the hole sector  $N_-(d^8)$  contribute  $J_{FM}(\vec{R}_{ij})$ , and all singlet states  $|nS\rangle$  contribute  $J_{AFM}(\vec{R}_{ij})$  to the exchange constant  $J_{tot}(\vec{R}_{ij})$ . Thus, the dependence of the superexchange interaction on the distance in the  $\text{CuO}_2$  layer can be calculated using  $t^{0,nS}(\vec{R}_{ij})$  and  $t^{0,mT}(\vec{R}_{ij})$  hopping integrals in Eq.(2).

### III. DIAGONAL SUPERXCHANGE INTERACTION IN A SQUARE SYMMETRY OF $\text{CuO}_2$ LAYER

Where are the effects of the  $\text{CuO}_2$  layer symmetry hidden in the calculation of  $J_{tot}(\vec{R}_{11})$  exchange constant using the Eq.(2)? To begin with, there is the point  $C_4$  symmetry of the  $\text{CuO}_6$  octahedron in the procedure of exact diagonalization of the intra-cell part of the Hamiltonian of the  $pd$  model <sup>33</sup>. Indeed, there are  $C_{2N_\lambda}^2 = N_S + 3N_T$  of the spin singlets  $N_S = C_{N_\lambda}^2 + N_\lambda$  and triplets  $N_T = C_{N_\lambda}^2$  in the two-hole  $N_-(d^8)$  sector (Fig.2) within  $N_\lambda$  orbital

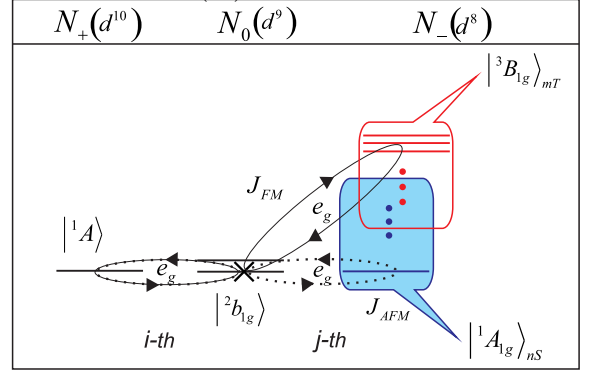


FIG. 2. Configuration space of the unit cell of the  $\text{CuO}_2$  layer. The cross denotes occupied hole eigenstates  $|b_{1g}\rangle$  in  $N_0(d^9)$  sector. The ellipses correspond to the virtual  $e_g$  electron-hole pairs with  $J_{FM}(\vec{R}_{ij})$  and  $J_{AFM}(\vec{R}_{ij})$  contributions to the total exchange interaction  $\hat{H}_S$ .

approach, where  $C_n^k$  is the number of combinations. For example, in the five-orbit approach there are 15 AFM ( $N_S = 15$ ) and 10 FM ( $N_T = 10$ ) contributions to the total superexchange interaction  $J_{tot}(\vec{R}_{ij})$  from various virtual electron-hole pairs.

Using the intracell part of the multi-orbital  $pd$  Hamiltonian in symmetric representation of canonical fermions <sup>35</sup> of the all spin singlet states  $|^1A_{1g}\rangle_{nS}$  and  $|^1B_{1g}\rangle_{mT}$ , spin triplet states  $|^3A_{1g}\rangle_{nS}$  and  $|^3B_{1g}\rangle_{mT}$ , and also single hole spin doublet states  $|^2a_{1g}\rangle, |^2b_{1g}\rangle$  can be obtained in the exact diagonalization procedure for the eigenvalue problem in the different sectors:  $N_-(d^8), N_0(d^9), N_+(d^{10})$  of configuration space. To solve the another problem associated with taking into account the common oxygen ion in the  $\text{CuO}_2$  layer, the initial  $pd$  Hamiltonian was rewritten in the representation of symmetrized Bloch  $2p$  states of oxygen ions<sup>31-33,35</sup>:

$$\begin{pmatrix} b_{\vec{k}\sigma} \\ a_{\vec{k}\sigma} \end{pmatrix} = \hat{P}(k_x, k_y) \begin{pmatrix} p_{x\vec{k}\sigma} \\ p_{y\vec{k}\sigma} \end{pmatrix} = i/\mu_{\vec{k}} \begin{pmatrix} s_x(\vec{k}) & s_y(\vec{k}) \\ \text{sgn}(k_x k_y) s_y(\vec{k}) & -\text{sgn}(k_x k_y) s_x(\vec{k}) \end{pmatrix} \begin{pmatrix} p_{x\vec{k}\sigma} \\ p_{y\vec{k}\sigma} \end{pmatrix}, \quad (5)$$

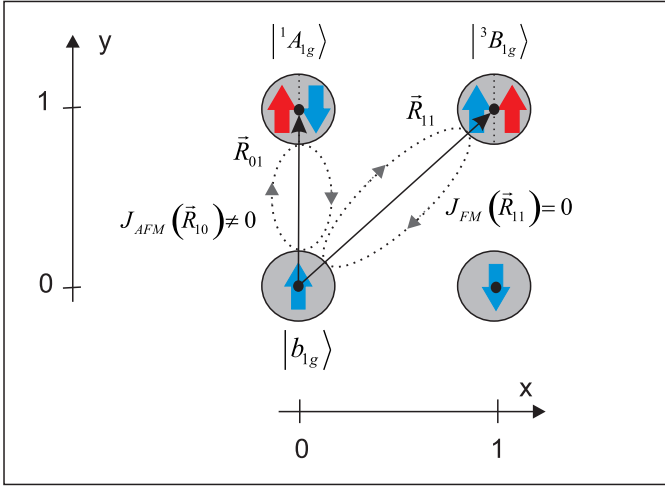


FIG. 3. A diagram of the direct and diagonal superexchange interactions at the cell representation in a simple square  $\text{CuO}_2$  layer. Here, ellipses shows the virtual electron-hole pairs with the contributions  $J_{FM}(\vec{R}_{ij})$  and  $J_{AFM}(\vec{R}_{ij})$  to the total superexchange interaction  $J_{tot}(\vec{R}_{ij})$ .

where  $|\hat{P}(k_x, k_y)|^2 = 1$ , and coefficients  $\mu_{\vec{k}} = \sqrt{s_x^2(\vec{k}) + s_y^2(\vec{k})}$  with  $s_x(\vec{k}) = \sin(k_x/2)$  and  $s_y(\vec{k}) = \sin(k_y/2)$  constructed on the square lattice of the  $\text{CuO}_2$  layer. As a consequence, the initial  $pd$  Hamiltonian in the cell representation of symmetrized Wannier states can be renormalized by using the coefficients  $\lambda_{\vec{k}} = \frac{2s_x s_y}{\mu_{\vec{k}}}$ ,  $\xi_{\vec{k}} = \frac{s_x^2 - s_y^2}{\mu_{\vec{k}}}$ , for  $pd$  hopping and  $\nu_{\vec{k}} = \frac{2s_x^2 s_y^2}{\mu_{\vec{k}}^2}$ ,  $\chi_{\vec{k}} = \frac{2s_x s_y}{\mu_{\vec{k}}^2} (s_x^2 - s_y^2)$  for  $pp$  hopping, two of which  $\xi(\vec{R}_{ij}) = \frac{1}{\sqrt{N}} \sum_{\vec{k}} \xi_{\vec{k}}$  and  $\chi(\vec{R}_{ij})$  are equal to zero for diagonal hopping with  $\vec{R}_{ij} = \vec{R}_{11}$ . Indeed, a square lattice remains invariant under replacement  $x \leftrightarrow y$ .

The symmetry of a virtual electron-hole pair in Fig.3 is determined by the symmetry of the  $|A_{1g}\rangle$  and  $|B_{1g}\rangle$  two-hole states, since a virtual electron can only be in the state  $|^1A\rangle$  of a completely occupied shell in the sector  $N_+$  (Fig.2). The coefficients  $\xi_{\vec{k}}$ ,  $\chi_{\vec{k}}$  renormalize only the contributions with holes at the  $|B_{1g}\rangle$  states, in the hopping Hamiltonian  $\hat{H}_1$

$$t_{\sigma}^{0,h}(\vec{R}_{ij}) \Big|_{h=|B_{1g}\rangle} = t^{p_x(p_y), d_{x^2}}(\vec{R}_{ij}) \xi(\vec{R}_{ij}) \times \dots + t^{p_x p_y}(\vec{R}_{ij}) \chi(\vec{R}_{ij}) \times \dots \doteq \begin{cases} 0 & , \vec{R}_{ij} = \vec{R}_{11} \\ \emptyset & , \vec{R}_{ij} = \vec{R}_{10} \end{cases} \quad (6)$$

and

$$t_{\sigma}^{0,h}(\vec{R}_{ij}) \Big|_{h=|A_{1g}\rangle} = t^{p_x(p_y), d_{x^2}}(\vec{R}_{ij}) \lambda(\vec{R}_{ij}) \times \dots + t^{p_x p_y}(\vec{R}_{ij}) \xi(\vec{R}_{ij}) \times \dots \neq 0 \quad (7)$$

at any  $\vec{R}_{ij}$ . Therefore, it is better to group the partial contributions to the total superexchange interaction  $\hat{H}_S$  not by their singlet or triplet spin nature, but by the orbital symmetry of the virtual electron-hole pair, which can be in different orbital states with  $A_{1g}$  and  $B_{1g}$  point symmetry (see Fig.3). Thus, instead of Eq.(2) we obtain

$$J_{tot}(\vec{R}_{ij}) = \Delta J_{AFM}^{A_{1g}}(\vec{R}_{ij}) + \Delta J_{FM}^{B_{1g}}(\vec{R}_{ij}), \quad (8)$$

where

$$\begin{aligned} \Delta J_{AFM}^{A_{1g}}(\vec{R}_{ij}) &= \sum_{n=1}^{N_S(^1A_{1g})} |t^{0,ns}(\vec{R}_{ij})|^2 / \Delta_{nS} - \quad (9) \\ &\quad - \sum_{m=1}^{N_T(^3A_{1g})} |t^{0,mT}(\vec{R}_{ij})|^2 / \Delta_{mT}, \\ \Delta J_{FM}^{B_{1g}}(\vec{R}_{ij}) &= \sum_{n=1}^{N_S(^1B_{1g})} |t^{0,ns}(\vec{R}_{ij})|^2 / \Delta_{nS} - \\ &\quad - \sum_{m=1}^{N_T(^3B_{1g})} |t^{0,mT}(\vec{R}_{ij})|^2 / \Delta_{mT}, \end{aligned}$$

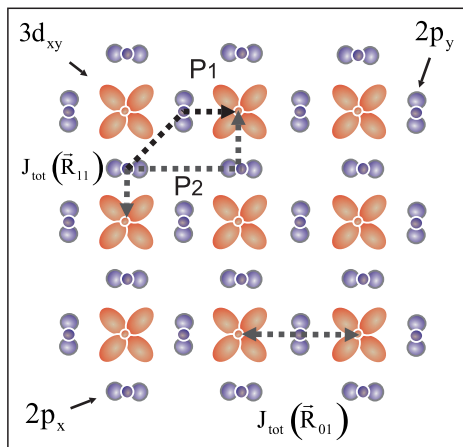


FIG. 4. Paths  $P_0$ ,  $P_1$  and  $P_2$  of superexchange interactions  $J_{tot}(\vec{R}_{01})$  and  $J_{tot}(\vec{R}_{11})$  for the nearest and next-nearest neighbors. Here, the oxygen  $2p$  orbitals  $\pi$ -overlap with  $t_{2g}$  magnetic ions, and form  $90^\circ$  ( $P_1$ ) and  $\sigma$  ( $P_2$ ) - overlapping between themselves. The interactions  $J_{tot}^{(P_1)}(\vec{R}_{11})$  and  $J_{tot}^{(P_2)}(\vec{R}_{11})$  are comparable in magnitude for the magnetic materials with partially occupied  $t_{2g}$  shell.

The contributions  $\Delta J_{AFM}^{A_{1g}}(\vec{R}_{ij})$  and  $\Delta J_{FM}^{B_{1g}}(\vec{R}_{ij})$  have AFM and FM nature, respectively, due to the levels of two-hole spin triplets  $|^3A_{1g}\rangle$  and singlets  $|^1B_{1g}\rangle$  lie higher in energy than the levels of spin singlets respectively. In fact, from Eq.(9), one finds

$$\begin{aligned} J_{tot}(\vec{R}_{01}) &= \Delta J_{AFM}^{A_{1g}}(\vec{R}_{01}) + \Delta J_{FM}^{B_{1g}}(\vec{R}_{01}) \approx (10.4 - 0.5) \times 10^{-2} eV = 9.9 \times 10^{-2} eV \\ J_{tot}(\vec{R}_{11}) &= \Delta J_{AFM}^{A_{1g}}(\vec{R}_{11}) + 0 \approx 0.2 \times 10^{-2} eV, \end{aligned} \quad (10)$$

where  $\Delta J_{AFM}^{A_{1g}}(\vec{R}_{01}) \approx (15.6 - 5.2) \times 10^{-2} = 10.4 \times 10^{-2} eV$ ,  $\Delta J_{FM}^{B_{1g}}(\vec{R}_{01}) \approx (0.4 - 0.9) \times 10^{-2} eV = -0.5 eV$  and  $\Delta J_{FM}^{B_{1g}}(\vec{R}_{11}) = 0$ , in the square  $\text{CuO}_2$  layer, due to an impossibility of diagonal mobility of the virtual holes at the two-hole state  $|B_{1g}\rangle$ . Consequently, there is only an AFM contribution to the diagonal superexchange  $J_{tot}(\vec{R}_{11})$  in Fig.3, due to the invariance of the square lattice under replacement  $x \leftrightarrow y$  with the magnetic ion  $\text{Cu}^{2+}$ .

#### IV. CONCLUSIONS

In summary, we have examined the sign and magnitude of superexchange interaction in  $\text{CuO}_2$  layer between next-nearest neighbors  $\text{Cu}^{2+}$  ions. At the LDA+GTB parameters<sup>36</sup> used before to calculate the energy structure and ARPES spectra HTSC cuprates we have obtained  $J_{tot}(\vec{R}_{11}) \approx 9.9 \times 10^{-2} eV$ . The diagonal  $J_{tot}(\vec{R}_{11})$  superexchange interaction in the simple square lattice of the  $\text{CuO}_2$  layer always has the AFM nature due to the symmetry prohibition on FM contribution  $\Delta J_{FM}^{B_{1g}}(\vec{R}_{11}) = 0$ . However, there isn't any prohibition  $\Delta J_{FM}^{B_{1g}}(\vec{R}_{01}) \approx -0.5 eV$  and  $\Delta J_{FM}^{A_{1g}}(\vec{R}_{01}) \approx 10.4 \times 10^{-2} eV$  for interacting nearest neighbors, and AFM exchange constant  $J_{tot}(\vec{R}_{ij})$  strongly decreases  $J_{tot}(\vec{R}_{11})/J_{tot}(\vec{R}_{01}) \approx 0.016$  with increasing distance between interacting  $\text{Cu}^{2+}$  ions.

In fact, we have confirmed that there are justified reasons to consider magnetic frustrations. However, one can expect the frustrations to be negligible for most part because of small ratio  $J_{tot}(\vec{R}_{11})/J_{tot}(\vec{R}_{01})$ . In the real  $\text{CuO}_2$  layer a breaking square symmetry can lead to the non-zero FM diagonal contribution  $\Delta J_{FM}^{B_{1g}}(\vec{R}) \neq 0$  supporting the smallness of this ratio. Therefore, a transfer of the results obtained for the pseudogap at the Mott transition in the triangular lattice Hubbard model with next-nearest-neighbor hopping and magnetic frustrations<sup>37</sup> to the square  $\text{CuO}_2$  layer are just motivating.

Note also, the models  $t - J$ ,  $t - t' - J$ ,  $t - t' - t'' - J$  with the extended hopping based on the single-band approach don't contain any FM contributions, and therefore correctly describe magnetic interactions only in a hypothetical square lattice, but not in the real  $\text{CuO}_2$  layer with broken square symmetry (e.g. with tilted  $\text{CuO}_6$  octahedra in D stripes<sup>38</sup>). In general, the type of magnetic ion remains clearly important in relation to the prohibition. This can be seen in Fig.4, where for magnetic ions with a partially occupied  $t_{2g}$  shell, the overlapping  $2p$  orbitals of oxygen ions along the path  $P_2$  is quite significant and should be taken into account to calculate the diagonal superexchange constant. A very interesting extension of this work would be to check an effect of certain type of broken square  $x \leftrightarrow y$  symmetry with unequal lattice parameters between the orthorhombic  $a$  and  $b$  axes on observed experimentally "Y shift" with surprisingly large tilt angle (so called diagonal stripes)<sup>10</sup>.

#### ACKNOWLEDGMENTS

We acknowledge the support of the Russian Science Foundation through grant RSF No.22-22-00298.

<sup>1</sup> J. F. Annett, R. M. Martin, A. K. McMahan, and S. Satpathy, Phys. Rev. B **40**, 2620 (1989).

<sup>2</sup> Y. J. Kim, A. Aharony, R. J. Birgeneau, F. C. Chou,

- O. Entin-Wohlman, R. W. Erwin, M. Greven, A. B. Harris, M. A. Kastner, I. Y. Korenblit, Y. S. Lee, and G. Shirane, Phys. Rev. Lett. **83**(4), 852 (1999).
- <sup>3</sup> R. Coldea, S. M. Hayden, G. Aeppli, T. G. Perring, C. D. Frost, T. E. Mason, S. W. Cheong, and Z. Fisk, Phys. Rev. Lett. **86**(23), 5377 (2001).
  - <sup>4</sup> V. A. Gavrichkov, S. I. Polukeev, and S. G. Ovchinnikov, Phys. Rev. B **95**, 144424 (2017).
  - <sup>5</sup> V. A. Gavrichkov, Z. V. Pchelkina, I. A. Nekrasov, and S. G. Ovchinnikov, International Journal of Modern Physics B **30**, 1650180 (2016).
  - <sup>6</sup> H. C. Jiang and T. P. Devereaux, Science **365**, 1424 (2019).
  - <sup>7</sup> S. R. White and D. J. Scalapino, Phys. Rev. B **60**, R753 (1999).
  - <sup>8</sup> C. M. Chung, M. Qin, S. Zhang, U. Schollwock, and S. R. White, Phys. Rev. B **102**, 041106 (2020).
  - <sup>9</sup> M. Qin, Phys. Rev. X **10**, 031016 (2020).
  - <sup>10</sup> W. He, J. Wen, H.-C. Jiang, G. Xu, W. Tian, T. Taniguchi, Y. Ikeda, M. Fujita, and Y. S. Lee, Commun Phys **7**, 257 (2024).
  - <sup>11</sup> S. Jiang, D. J. Scalapino, and S. R. White, Phys. Rev. B **106**, 174507 (2022).
  - <sup>12</sup> M. Hartstein, Y. Hsu, K. A. Modic, J. Porras, T. Loew, M. LeTacon, H. Zuo, J. Wang, Z. Zhu, M. K. Chan, R. D. McDonald, G. G. Lonzarich, B. Keimer, S. E. Sebastian, and N. Harrison, Nature Physics **16**, 841–847 (2020).
  - <sup>13</sup> A. Kanigel, M. R. Norman, M. Randeria, U. Chatterjee, S. Souma, A. Kaminski, H. M. Fretwell, S. Rozenkranz, M. Shi, T. Sato, T. Takahashi, Z. Z. Li, H. Raffy, K. Kadowaki, D. Hinks, L. Ozyuzer, and C. J. C, Nature Physics **2**, 447 (2006).
  - <sup>14</sup> H. Al-Rashid and D. K. Singh, SciPost Phys. **16**, 107 (2024).
  - <sup>15</sup> K. S. Chen, Z. Y. Meng, T. Pruschke, J. Moreno, and M. Jarrell, Phys. Rev. B **86**, 165136 (2012).
  - <sup>16</sup> M. Kohno, Phys. Rev. B **90**, 035111 (2014).
  - <sup>17</sup> E. Gull, O. Parcollet, P. Werner, and A. J. Millis, Phys. Rev. B **80**, 245102 (2009).
  - <sup>18</sup> S. Wakimoto, Phys. Rev. B **60**, R769 (1999).
  - <sup>19</sup> F. M., Phys. Rev. B **65**, 064505 (2002).
  - <sup>20</sup> S. R. Dunsiger, Phys. Rev. B **78**, 092507 (2008).
  - <sup>21</sup> V. A. Gavrichkov, S. I. Polukeev, and S. G. Ovchinnikov, Phys. Rev. B **101**, 094409 (2020).
  - <sup>22</sup> R. V. Mikhaylovskiy, T. J. Huisman, V. A. Gavrichkov, S. I. Polukeev, S. G. Ovchinnikov, D. Afanasiev, R. V. Pisarev, T. Rasing, and K. A. V, Phys. Rev. Lett. **125**, 157201 (2020).
  - <sup>23</sup> H. Kamimura and M. Eto, J. Phys. Soc. Jpn **59**, 3053 (1990).
  - <sup>24</sup> M. Eto and H. Kamimura, Physica C Superconductivity **185–189**, 1599–1600 (1991).
  - <sup>25</sup> C. Janowitz, U. Seidel, R.-S. T. Unger, A. Krapf, R. Manzke, V. Gavrichkov, and S. Ovchinnikov, JETP Letters **80**(11), 692 (2004).
  - <sup>26</sup> P. W. Anderson, Phys. Rev. **115**, 2 (1959).
  - <sup>27</sup> K. A. Chao, J. Spalek, and A. M. Oles, Journal of Physics C: Solid State Physics **10**, L271 (1977).
  - <sup>28</sup> J. Hubbard, Proc. Roy. Soc. **A276**, 238 (1963).
  - <sup>29</sup> S. G. Ovchinnikov and V. V. Val'kov, *Hubbard operators in the theory strongly correlated electrons* (Imperial College Press, London, 2004) p. 241.
  - <sup>30</sup> S. G. Ovchinnikov, V. A. Gavrichkov, M. M. Korshunov, and E. I. Shneyder, “Springer series in solid-state sciences,” (Volume 171, Springer Berlin Heidelberg, Hamburg, 2012) Chap. LDA+GTB method for band structure calculations in the strongly correlated materials. In the “Theoretical Methods for strongly Correlated systems”, pp. 143–171.
  - <sup>31</sup> L. F. Feiner, J. H. Jefferson, and R. Raimondi, Phys. Rev. B **53**, 8751 (1996).
  - <sup>32</sup> L. F. Feiner, J. H. Jefferson, and R. Raimondi, Phys. Rev.Lett. **76**, 4939 (1996).
  - <sup>33</sup> V. A. Gavrichkov, S. G. Ovchinnikov, A. A. Borisov, and E. G. Goryachev, Journal of Experimental and Theoretical Physics **91**(2), 369 (2000).
  - <sup>34</sup> V. Y. Irkhin and Y. P. Irkhin, Phys. Status Solidi B **183**, 9 (1994).
  - <sup>35</sup> B. S. Shastry, Phys. Rev. Lett. **63**, 1288 (1989).
  - <sup>36</sup> M. M. Korshunov, V. A. Gavrichkov, S. G. Ovchinnikov, I. A. Nekrasov, Z. V. Pchelkina, and V. I. Anisimov, Phys. Rev. B **72**, 165104 (2005).
  - <sup>37</sup> P. O. Downey, O. Gingras, J. Fournier, C. D. Hebert, M. Charlebois, and A.-M. S. Tremblay, Phys. Rev. B **107**, 125159 (2023).
  - <sup>38</sup> A. Bianconi, N. L. Saini, A. Lanzara, M. Missori, T. Rossetti, H. Oyanagi, H. Yamaguchi, K. Oka, and T. Ito, Phys. Rev. Lett. **76**, 3412 (1996).